GeroScience (2023) 45:1745–1759
https://doi.org/10.1007/s11357-023-00726-4

ORIGINAL ARTICLE

Growth hormone receptor (GHR) in AgRP neurons regulates thermogenesis in a sex-specific manner

Lukas Stilgenbauer · Juliana Bezerra Medeiros de Lima · Lucas Kniess Debarba · Manal Khan · Lisa Koshko · John J. Kopchick · Andrzej Bartke · Augusto Schneider · Marianna Sadagurski

Received: 27 August 2022 / Accepted: 3 January 2023 / Published online: 12 January 2023

Abstract Evidence for hypothalamic regulation of energy homeostasis and thermoregulation in brown adipose tissue (BAT) during aging has been well recognized, yet the central molecular mediators involved in this process are poorly understood. The arcuate hypothalamus, orexigenic agouti–related peptide (AgRP) neurons control nutrient intake, energy homeostasis, and BAT thermogenesis. To determine the roles of growth hormone receptor (GHR) signaling in the AgRP neurons, we used mice with the AgRP-specific GHR deletion ($AgRP^{\Delta GHR}$). We found that female $AgRP^{\Delta GHR}$ mice were resistant to temperature adaptation, and their body core temperature remained significantly lower when held at 10 °C, 22 °C, or 30 °C, compared to control mice. Low body core temperature in female $AgRP^{\Delta GHR}$ mice has been associated with significant reductions in *Ucp1* and *Pgc1α* expression in the BAT. Further, neuronal activity in AgRP in response to cold exposure was blunted in $AgRP^{\Delta GHR}$ female mice, while the number of Fos^{+} AgRP neurons was increased in female controls exposed to cold. Global transcriptome from BAT identified increased the expression of genes related to immune responses and chemokine activity and decreased the expression of genes involved in triglyceride synthesis and metabolic pathways in $AgRP^{\Delta GHR}$ female mice. Importantly, these were the same genes that are downregulated by thermoneutrality in control mice but not in the $AgRP^{\Delta GHR}$ animals. Collectively, these data demonstrate a novel sex-specific role for GHR signaling in AgRP neurons in thermal regulation, which might be particularly relevant during aging.

Keywords Growth hormone receptor · Thermoregulation · Aging · AgRP neurons

Abbreviations

AgRP	Agouti-related peptide
ARC	Arcuate nucleus
BAT	Brown adipose tissue
CNS	Central nervous system

Lukas Stilgenbauer and Juliana Bezerra Medeiros de Lima contributed equally to this study.

Supplementary Information The online version contains supplementary material available at https://doi.org/10.1007/s11357-023-00726-4.

L. Stilgenbauer · J. B. M. de Lima · L. K. Debarba · M. Khan · L. Koshko · M. Sadagurski (✉)
Department of Biological Sciences, Integrative Biosciences Center (IBio), Wayne State University, 6135 Woodward, Detroit, MI 48202, USA
e-mail: sadagurski@wayne.edu

J. J. Kopchick
Edison Biotechnology Institute, Ohio University, Athens, OH, USA

A. Bartke
Department of Internal Medicine, Southern Illinois University School of Medicine, Springfield, USA

A. Schneider
Nutrition College, Federal University of Pelotas, Pelotas, Rio Grande Do Sul, Brazil

DMH	Dorsomedial hypothalamic nucleus
GH	Growth hormone
GHR	Growth hormone receptor
GHRH	Growth hormone–releasing hormone
LHA	Lateral hypothalamus
POMC	Proopiomelanocortin
PVH	Paraventricular hypothalamic nucleus

Introduction

During aging, brown adipose tissue (BAT) loses its thermogenic capacity and adaptation to cold temperatures, thus reducing its ability to maintain normal energy homeostasis and body temperature late in life [1]. Energy homeostasis and thermoregulation are coordinated in the arcuate nucleus (ARC) of the hypothalamus, which integrates neuronal and hormonal signals originating from peripheral tissues [2]. In the ARC, an antagonistic interaction between neurons expressing agouti-related peptide (AgRP) and neurons expressing proopiomelanocortin (POMC) constitutes the central metabolic controlling axis, and alterations in its activity impair energy homeostasis, thermoregulation, and peripheral glucose metabolism [3, 4]. Age-associated alterations in thermoregulation include low heat production, impaired thermal perception, and impaired autonomic and thermoregulatory responses [5]. Shivering is critical for heat production in a cold environment. Compared to young adults, shivering to increase heat production is impaired in elderly people and in laboratory animals, which reduces their tolerance for cold environments [6, 7].

In the hypothalamus, thermoregulatory circuits are modulated by leptin- and insulin-sensing neurons that respond to external nutrient and temperature cues [8]. Hypothalamic leptin and insulin signaling influence baselines of body core temperature in the fed state and oppose entry into a torpor-like state, without an effect on thermogenic response to cold [8]. In general, the preoptic area (POA) of the hypothalamus is responsible for managing body temperature; however, a subset of AgRP neurons was recently identified to mediate thermogenesis [9, 10]. In support, female mice lacking corticotropin-releasing factor receptor type 1 (CRFR1) selectively in AgRP neurons exhibit a maladaptive thermogenic response to cold following impaired activation of the sympathetic nervous system (SNS) [11].

Growth hormone (GH) is a key mediator of growth and metabolism [12, 13]. GH-deficient, long-lived Ames dwarf mice have highly active BAT compared to their littermates as indicated by depleted lipid stores, increased BAT tissue weight, increased expression of genes related to thermogenesis and lipid metabolism, and increased oxygen consumption and energy expenditure [14–16]. Housed Ames dwarf mice at thermoneutrality normalize their lipid stores, gene expression, and oxygen consumption compared to control mice [14, 15], suggesting that changes in BAT correlated with the extended longevity of GH-deficient mice.

GH activates AgRP neurons [17]. We and others have shown that young mice carrying AgRP-specific GHR ablation ($AgRP^{\Delta GHR}$ mice) have similar body weight, food intake, hormonal levels, and insulin sensitivity compared to control animals [17, 18]. However, during fasting, AgRP neurons' ability to save energy is impaired in AgRP GHR KO male mice, leading to increased fat loss, indicating GH as a starvation signal in AgRP neurons [17]. Given the role GH signaling plays in aging and its effect on BAT thermogenic capacity, in the current study, we used $AgRP^{\Delta GHR}$ mice to explore the role of GHR signals in AgRP neurons in thermoregulation and thermoregulatory responses to temperature cues in aging animals.

Materials and methods

Animals

Adult male and female $AgRP^{tm1(cre)}$ (AgRP-Ires-cre, stock 012899) mice were purchased from the Jackson Laboratory, and $GHR^{L/L}$ mice were described previously [19]. The characterization of the $AgRP^{\Delta GHR}$ mice was described previously [18]. We used wild-type control littermates whenever possible, and if not available, we used age-matched controls from the same breeding line. All mice were provided ad libitum access to a standard chow diet (Purina Lab Diet 5001) and housed in temperature-controlled rooms on a 12-h/12-h light–dark cycle. Procedures involved in this study were approved by the Wayne State

University Institutional Animal Care and Use Committee (IACUC).

Temperature exposure and core body temperature monitoring

Mice were anesthetized using isoflurane. A mid-sagittal incision was made in the abdomen, and a passive radio frequency identification (RFID) chip was inserted into the abdominal fat pat. Mice were monitored three times daily with RFID readers for core body temperature. Mice were housed at 22 °C for 2 days before the temperature challenge to allow them to equilibrate. After 2 days of equilibration, the mice were then monitored for 2 days at 22 °C followed by 3 days at 10 °C, 2 days at 22 °C, and 3 days at 30 °C. Metabolic measurements of energy homeostasis at 22 °C were obtained using an indirect calorimetry system (PhenoMaster, TSE system; Bad Homburg, Germany). The mice were acclimatized to the cages for 2 days and monitored for 5 days while food and water were provided ad libitum.

Perfusion and immunolabeling

Mice were anesthetized and perfused using phosphate-buffered saline (PBS) (pH 7.5) followed by 4% paraformaldehyde (PFA). Brains were post-fixed, dehydrated, and sectioned coronally (30 µm) using a sliding microtome, followed by immunofluorescent analysis as described [20]. For immunohistochemistry, brain sections were washed with PBS six times, blocked with 0.3% Triton X-100 and 3% normal donkey serum in PBS for 2 h; then, the staining was carried out with the mouse anti-cFos (anti-rabbit, 1:500, cat. number sc-52; Santa Cruz). Immunostained brain sections were pretreated with 0.5% NaOH and 0.5% H_2O_2 in PBS for 20 min. After the primary antibody treatment, brain sections were incubated with Alexa Fluor–conjugated secondary antibodies for 2 h (Invitrogen). Microscopic images of the stained sections were obtained using Olympus FluoView 500 and Zeiss LSM 800 laser scanning confocal microscopes.

Quantification

For the quantification of immunoreactivity, images of matched brain areas were taken from at least 3 sections containing the hypothalamus for each brain between the bregma − 0.82 and − 2.4 mm (according to the Franklin mouse brain atlas). Serial brain sections were made at 30 µm thickness, and every five sections were represented by one section with staining and cell counting. All sections were arranged from rostral to caudal to examine the distribution of labeled cells. $cFos^+$ cells were counted using ImageJ with DAPI (nuclear staining). The average of the total number of cells/field was assessed by statistical analysis as detailed in the following section.

Quantitative real-time PCR

Total RNA was isolated from dissected BAT using TRIzol reagent (Invitrogen, #15596026). The concentration of 1000 ng of RNA was used for complementary DNA (cDNA) synthesis using the High Capacity cDNA Reverse Transcription Kit (Bio-Rad, #1708891). To detect the contaminated DNA, we used the samples processed without the reverse transcriptase enzymes as negative controls. Quantitative real-time PCR was performed using the Applied Biosystems 7500 Real-Time PCR System (PGC1α, forward: GCAACATGCTCAAGCCAAAC and reverse: TGCAGTTCCAGAGAGTTCCA; Ucp1, forward: GCTTTGCCTCACTCAGGATTGG and reverse: CCAATGAACACTGCCACACCTC; FGF21, forward: CCTCTAGGTTTCTTTGCCAACAG and reverse: AAGCTGGCCTCAGGAT). Each PCR reaction was performed in duplicate. As negative controls, we used water instead of the cDNA, and β-actin was measured in each cDNA sample as the housekeeping gene. The ΔΔCT method was used to determine the gene transcripts in each sample. For each sample, the threshold cycle (CT) was measured and normalized to the average of the housekeeping gene (ΔCT = CT gene of interest − CT housekeeping gene). The fold change of messenger RNA (mRNA) in the rest of the samples relative to the male control group was determined by $2^{-\Delta\Delta CT}$. Data are shown as mRNA expression levels relative to the male controls.

Histology and morphometric analysis

Histological analysis was performed on BAT tissues isolated from the animals at room temperature, or exposed to 10 °C, or at 30 °C as previously described [21]. Morphometric analysis of BAT was performed with NIH ImageJ software (http://rsb.info.nih.gov/ij/).

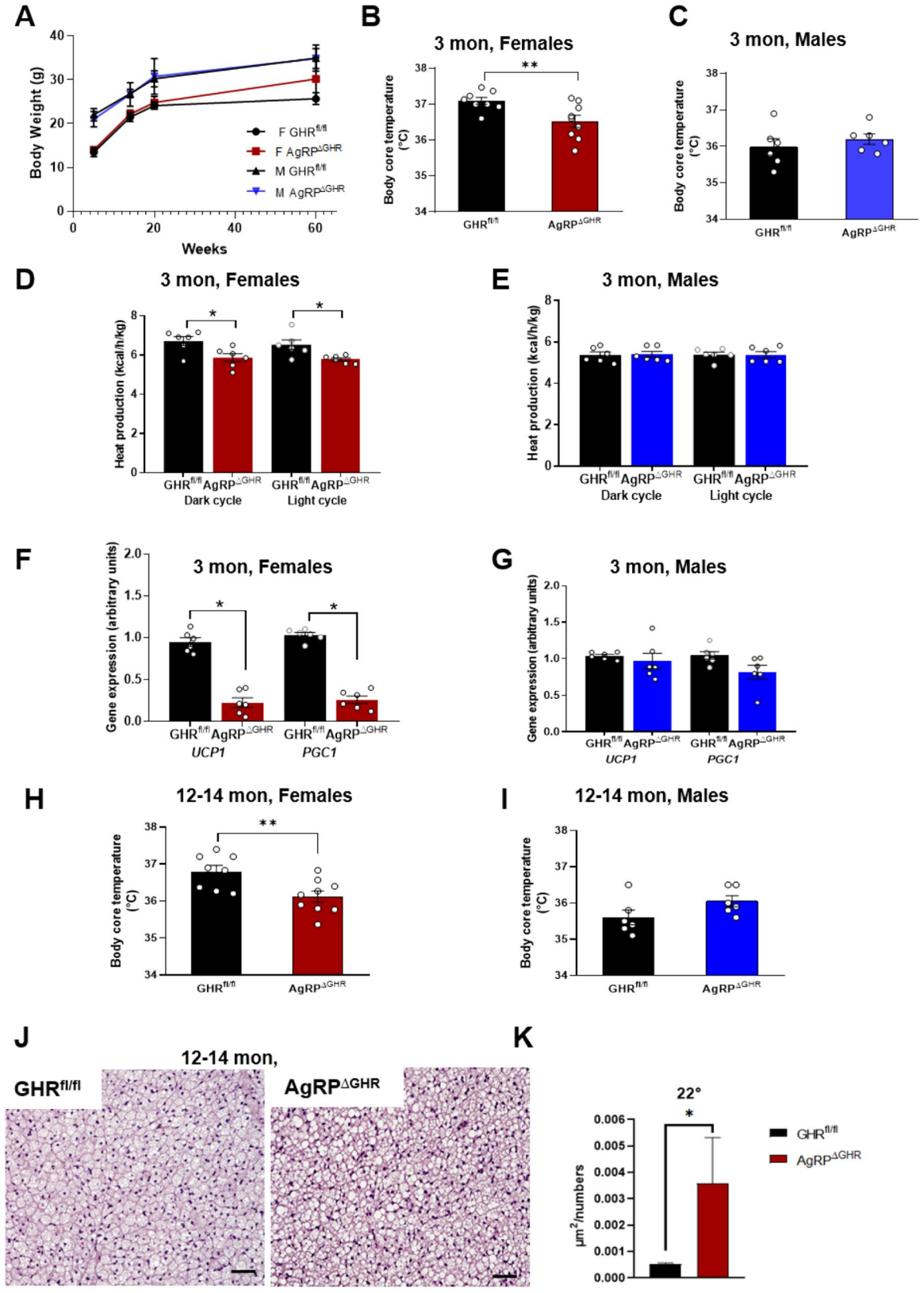
A
Body Weight (g)
Weeks
F GHR fl/fl
F AgRP ΔGHR
M GHR fl/fl
M AgRP ΔGHR
B
3 mon, Females
Body core temperature (°C)
GHR fl/fl
AgRP ΔGHR
C
3 mon, Males
D
3 mon, Females
Heat production (kcal/h/kg)
Dark cycle
Light cycle
E
3 mon, Males
F
3 mon, Females
Gene expression (arbitrary units)
UCP1
PGC1
G
3 mon, Males
H
12-14 mon, Females
I
12-14 mon, Males
J
12-14 mon,
GHR fl/fl
AgRP ΔGHR
K
22°
μm²/numbers

◂**Fig. 1** Temperature control in AgRP$^{\Delta GHR}$ mice. **A** Body weight. Body core temperature of 12-week-old female (**B**) and male (**C**) control and AgRP$^{\Delta GHR}$ mice. Energy parameters were measured in ad libitum control and AgRP$^{\Delta GHR}$ mice. Heat production in female (**D**) and male (**E**) mice. Gene expression of *UCP1* and *PGC1* in BAT of 12-week-old female (**F**) and male (**G**) mice ($n=6$). Data are shown as mean ± SEM. *$p<0.001$. Body core temperature of 12–14-month-old female (**H**) and male (**I**) control and AgRP$^{\Delta GHR}$ mice ($n=7$–8). Representative images (**J**) and quantification (**K**) of H&E staining in BAT of 12–14-month-old female mice ($n=6$). Data are shown as mean ± SEM. *$p<0.05$. See also Supplementary Fig. 1

RNA extraction and mRNA sequencing

RNA sequencing (RNA-Seq) was performed at the WSU Genome Sciences Core. All RNA-Seq data processing was performed as before [22]. Transcriptomic profile of individual BAT samples was performed using commercial RNA sequencing kits (NEBNext mRNA Library Prep Master Mix and NEBNext Multiplex Oligos for Illumina, New England Biolabs, Ipswich, MA, USA) and adapted according to previous descriptions [22]. All RNA-Seq data are available at the Sequence Read Archive (SRA) at NCBI under accession number PRJNA871915. The mapping of sequencing reads to the mouse transcriptome and mRNA abundance was performed as previously [22]. mRNAs were further processed for pathway analysis using the generally applicable gene set enrichment (GAGE), for the enrichment of KEGG pathways and Gene Ontology (GO) terms (biological processes, molecular function, and cellular component).

Statistical analysis

Statistical analyses for differentially expressed mRNAs were performed pairwise using EdgeR in the software R (3.2.2). Genes with a false discovery rate (FDR) < 0.05 and fold change (FC) > 2.0 were considered upregulated, and those with an FDR < 0.05 and FC < 0.5 were considered downregulated. For all other experiments, the unpaired two-tailed Student's *t* test was used for comparisons between two groups. Statistical analyses were performed using the GraphPad Prism software. A *p* value of less than 0.05 was considered statistically significant.

Results

Female AgRP$^{\Delta GHR}$ mice exhibit decreased body core temperature

AgRP$^{\Delta GHR}$ mice show no difference in body weight as compared to control littermates (Fig. 1A), although by 14 months of age, female AgRP$^{\Delta GHR}$ mice demonstrated a slight, but insignificant ($p=0.056$), gain in body weight (Fig. 1A). By 12 weeks of age, female, but not male, AgRP$^{\Delta GHR}$ mice exhibited reduced body core temperature compared to controls (Fig. 1B, C). The body core temperature was overall higher in female mice, consistent with previous reports [23]. Additionally, when placed in metabolic chambers, female AgRP$^{\Delta GHR}$ mice exhibited a reduction in heat production without differences in the respiratory exchange ratio (RER) or ambulatory activity levels (Fig. 1D and Supplementary Fig. 1). These data are in agreement with a previous report showing that young AgRP$^{\Delta GHR}$ male mice exhibited no differences in heat production, RER, or activity levels (Fig. 1E and Supplementary Fig. 1) [17]. Gene expression analysis of BAT demonstrated reduced levels of *Ucp1* (mitochondrial uncoupling protein 1) and *Pgc1α* (peroxisome proliferator–activated receptor gamma, co-activator 1 alpha (Ppargc1α)) in 3-month-old female AgRP$^{\Delta GHR}$ mice compared to control littermates (Fig. 1F). We did not detect differences in the expression levels of *Ucp1* and *Pgc1α* in male AgRP$^{\Delta GHR}$ mice compared to controls (Fig. 1G). Interestingly, as found at a young age, 12–14-month-old female AgRP$^{\Delta GHR}$ mice exhibited decreased body core temperature compared to controls. No differences were detected in body core temperature in male AgRP$^{\Delta GHR}$ mice (Fig. 1H, I). Histological examination of BAT (H&E-stained sections) revealed a significant increase in lipid droplet size in brown adipocytes in young and middle-aged female AgRP$^{\Delta GHR}$ mice (Fig. 1J, K, and Supplementary Fig. 1C, D).

Remodeling of BAT transcription in adult AgRP$^{\Delta GHR}$ female mice

To further investigate age-related aberrations in BAT, we performed bulk RNA-Seq of the BAT from 14-month-old female AgRP$^{\Delta GHR}$ mice and compared it to female controls. Results of principal component analysis for the most variable genes and hierarchical

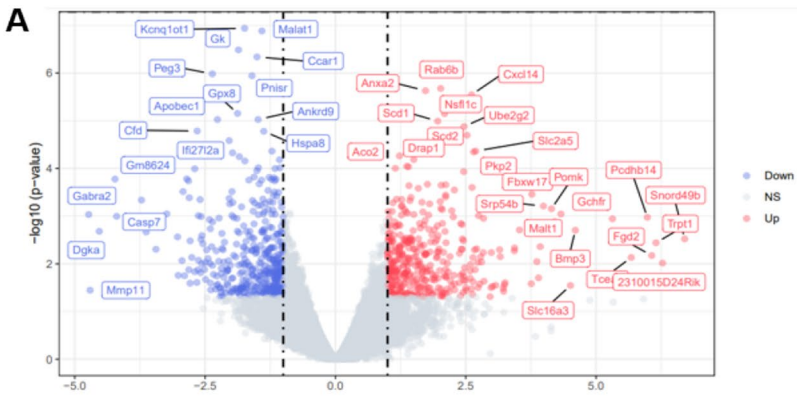
A
Kcnq1ot1
Gk
Malat1
Ccar1
Peg3
Gpx8
Pnisr
Apobec1
Ankrd9
Cfd
Hspa8
Ifi27l2a
Gm8624
Gabra2
Casp7
Dgka
Mrnp11
Rab6b
Cxcl14
Anxa2
Nsfl1c
Scd1
Ube2g2
Scd2
Slc2a5
Aco2
Drap1
Pkp2
Fbxw17
Pomk
Pcdhb14
Snord49b
Srp54b
Gchfr
Trpt1
Malt1
Fgd2
Bmp3
Tce
2310015D24Rik
Slc16a3
−log10 (p-value)
Down
NS
Up

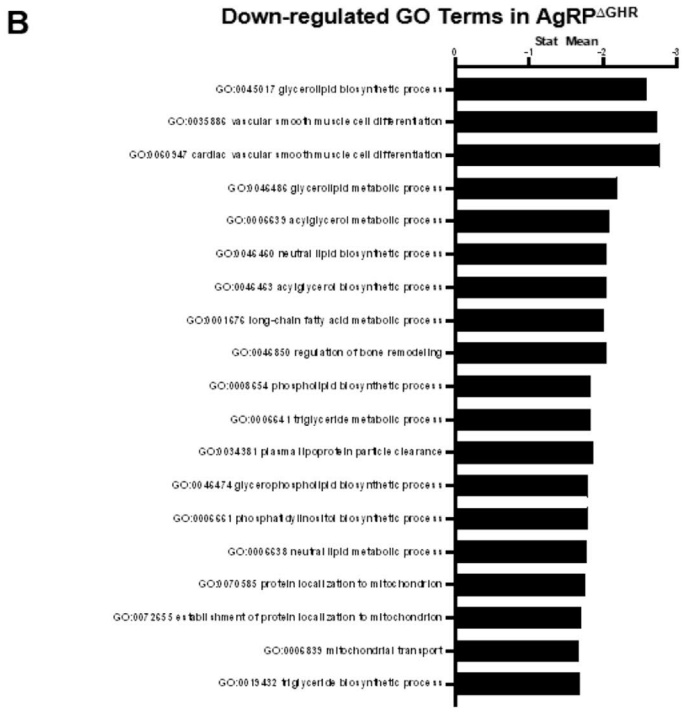
B
Down-regulated GO Terms in AgRP^ΔGHR
Stat Mean
GO:0045017 glycerolipid biosynthetic process
GO:0035886 vascular smooth muscle cell differentiation
GO:0060947 cardiac vascular smooth muscle cell differentiation
GO:0046486 glycerolipid metabolic process
GO:0006639 acylglycerol metabolic process
GO:0046460 neutral lipid biosynthetic process
GO:0046463 acylglycerol biosynthetic process
GO:0001676 long-chain fatty acid metabolic process
GO:0046850 regulation of bone remodeling
GO:0008654 phospholipid biosynthetic process
GO:0006641 triglyceride metabolic process
GO:0034381 plasma lipoprotein particle clearance
GO:0046474 glycerophospholipid biosynthetic process
GO:0006661 phosphatidylinositol biosynthetic process
GO:0006638 neutral lipid metabolic process
GO:0070585 protein localization to mitochondrion
GO:0072655 establishment of protein localization to mitochondrion
GO:0006839 mitochondrial transport
GO:0019432 triglyceride biosynthetic process

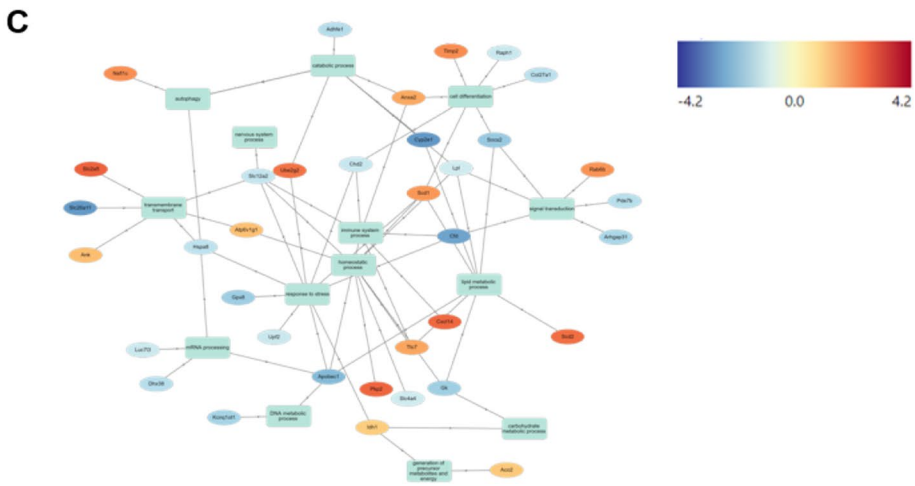
C
-4.2
0.0
4.2

◂**Fig. 2** BAT transcription profile in adult AgRP$^{\Delta GHR}$ female mice. **A** Volcano plot of the differential expression of genes in 12–14-month-old AgRP$^{\Delta GHR}$ female mice compared to female controls. The blue, red, and gray dots represent the downregulated, upregulated, and unchanged genes, respectively. **B** Downregulated functions identified by GO analysis. **C** Network analysis of differentially expressed genes associated with carbohydrate metabolic process, lipid metabolic process, immune system, homeostatic process, and stress response. Red and blue colors indicate upregulated and downregulated genes compared to the control group. See also Supplementary Fig. 2 and Supplementary Tables 1, 2, and 3 for analysis of pathways

clustering in BAT identified a clear separation for controls vs. AgRP$^{\Delta GHR}$ animals (Supplementary Fig. 2). Volcano plot shows the main upregulated and downregulated genes in female AgRP$^{\Delta GHR}$ mice relative to the controls (Fig. 2A). The complete list of regulated pathways is presented in Supplementary Tables 1, 2, and 3. Of particular interest, the number of lipid metabolic pathways, including triglyceride metabolism, glycerolipid metabolism, acylglycerol biosynthesis, lipid and phospholipid biosynthesis, and isocitrate metabolism, was significantly downregulated in BAT from female AgRP$^{\Delta GHR}$ mice as compared to the controls (Fig. 2B). Among the genes associated with lipid metabolic processes and glucose regulation, *Apobec1*, *Cyp2e1*, *Gk*, *Malat1*, *Ankrd9*, *Kcnq1ot1*, *Slc12a2*, and *Lpl* were downregulated, while among the genes associated with fatty acid metabolism, *Scd1* and *Scd2* were upregulated (Fig. 2C).

AgRP$^{\Delta GHR}$ female mice do not adapt to changes in temperature

To further investigate the requirement of GHR in AgRP neurons for adaptation to cold or at thermoneutrality, we recorded body core temperature during the light cycle in middle-aged, 12–14-month-old female mice exposed for 3 days to 10 °C or 30 °C and compared the outcomes to those measured in mice housed at room temperature (22 °C) (Fig. 3A). Using this exposure paradigm, we found profound differences in sensitivity to cold and thermoneutrality between control and AgRP$^{\Delta GHR}$ female mice. Female controls maintained their body temperature at 10 °C, while female AgRP$^{\Delta GHR}$ mice exhibited a significantly lower body core temperature upon exposure to 10 °C, as compared to controls (Fig. 3B). Furthermore, housing mice for 3 days at thermoneutrality (30 °C), where cold-induced thermogenesis is minimal, did not normalize the body core temperature of female AgRP$^{\Delta GHR}$ mice that was maintained consistently lower than that of controls (Fig. 3C). Interestingly, middle-aged male AgRP$^{\Delta GHR}$ mice showed adaptation to changes in temperature that was similar to that of their control littermates (Fig. 3D, E, and Supplementary Fig. 3). Total body weight was unaffected (data not shown); however, the sustained cold exposure or thermoneutrality resulted in pronounced changes in BAT morphology in control animals. H&E-stained BAT from female mice housed at ambient temperature had brown adipocytes with multiple small lipid droplets, while BAT from female AgRP$^{\Delta GHR}$ mice had significantly larger single-lipid droplets (Fig. 3F, G). In contrast, H&E-stained BAT from cold-exposed female control mice showed much smaller brown adipocytes and fewer lipid droplets than at 22 °C ($p < 0.00001$ for effect of temperature), indicating that cold exposure induced a loss of lipid droplets in the brown adipocytes (Fig. 3F). We did not detect significant cold-induced morphological changes in female AgRP$^{\Delta GHR}$ mice compared to controls (Fig. 3F, H). Regardless, *Ucp1* and *Pgc1* expression levels increased with cold temperature in control but not in female AgRP$^{\Delta GHR}$ mice. Importantly, the expression levels of *Ucp1* and *Pgc1* were downregulated in the female AgRP$^{\Delta GHR}$ mice housed at room temperature and maintained low regardless of the temperature change (Fig. 3I). Interestingly, the expression levels of *Fgf21* were also significantly elevated in response to cold exposure in control mice, supporting its activation by cold [24], while *Fgf21* levels were significantly reduced in cold but elevated at 30 °C in female AgRP$^{\Delta GHR}$ mice, suggesting transcriptional dysregulation of *Fgf21* in BAT.

ARC neurons do not adapt to cold exposure in female AgRP$^{\Delta GHR}$ mice

A recent study demonstrated that mild cold exposure induces activation of cFos protein, a marker of neuronal activation in AgRP neurons [25]. We found that the total number of cFos^{+} neurons in the ARC was comparable in both control and AgRP$^{\Delta GHR}$ female mice maintained at 22 °C. However, the number of cFos^{+} neurons was significantly increased in response to cold exposure in control, but not in female AgRP$^{\Delta GHR}$ mice (Fig. 4A, B). A similar effect was

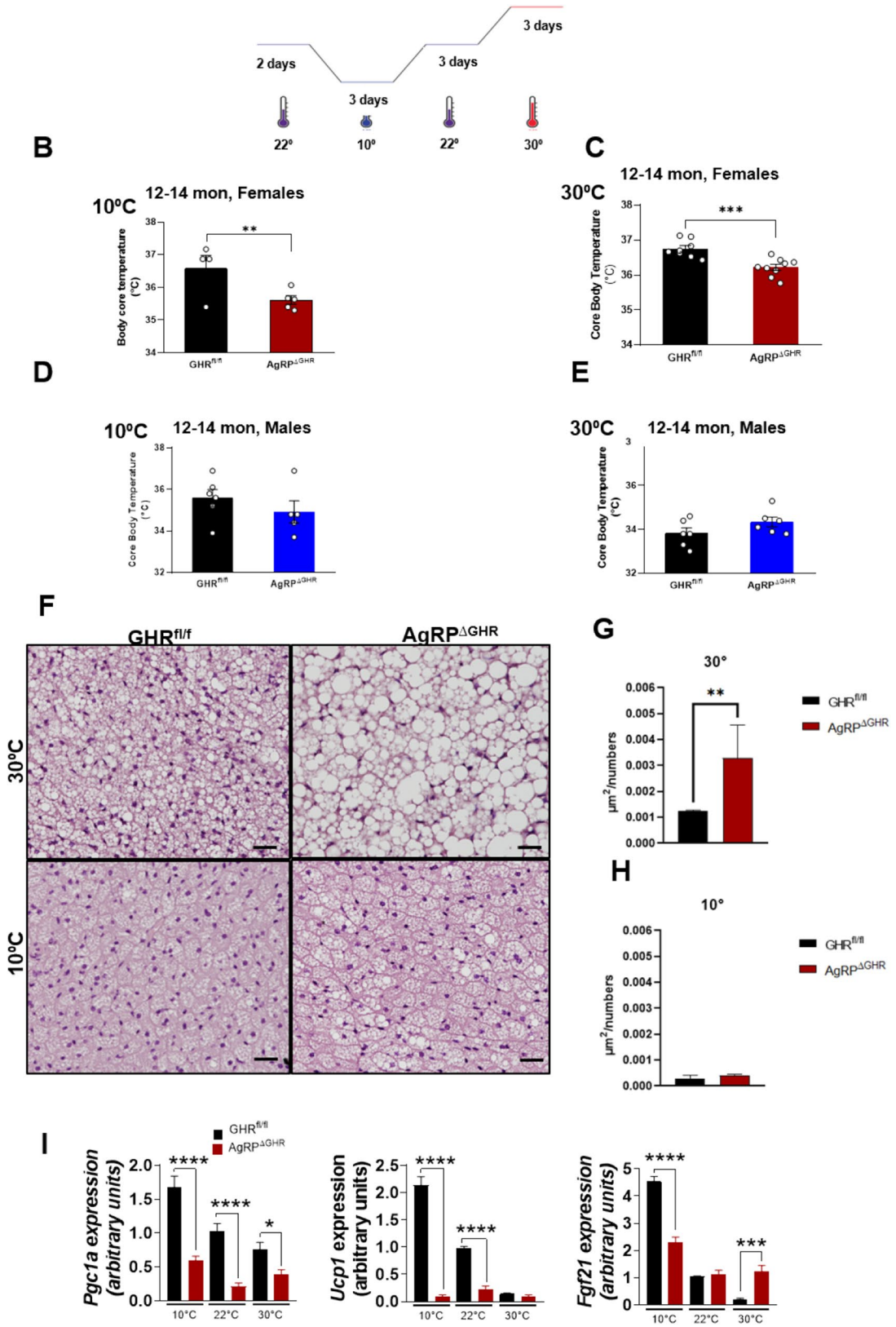
2 days
3 days
3 days
3 days
22°
10°
22°
30°
B
C
10°C
12-14 mon, Females
Body core temperature (°C)
**
GHRfl/fl
AgRP∆GHR
30°C
12-14 mon, Females
Core Body Temperature (°C)
***
D
E
10°C
12-14 mon, Males
30°C
12-14 mon, Males
F
GHRfl/f
AgRP∆GHR
30°C
10°C
G
30°
**
µm2/numbers
H
10°
I
Pgc1a expression (arbitrary units)
Ucp1 expression (arbitrary units)
Fgf21 expression (arbitrary units)
****
*
***
10°C
22°C
30°C

◂**Fig. 3** Effect of cold exposure or thermoneutrality on body core temperature and BAT gene expression. **A** Control and AgRP$^{\Delta GHR}$ female and male mice aged 12–14 months were housed in temperature-controlled chambers set to either 10 °C (cold) or 30 °C for 3 days. Body core temperature in female (**B**) and male (**D**) mice housed at 10 °C. Body core temperature in female (**C**) and male (**E**) mice housed over 3 days at 30 °C. $n = 5$–8 per group, mean ± SEM. Student's t test, $^{*}p < 0.05$. Representative images (**F**) and quantification (**G** and **H**) of H&E staining in BAT of 12–14-month-old female mice housed at 10 °C or 30 °C for 3 days ($n = 6$), t test, $^{*}p < 0.05$, $^{**}p < 0.01$. See also Supplementary Fig. 3 for H&E staining in BAT of 12–14-month-old male mice. **I** Gene expression of *PGC1*, *UCP1*, and *Fgf21* in BAT of 12–14-month-old control and AgRP$^{\Delta GHR}$ female mice housed at 22 °C, 10 °C, or 30 °C as determined by qRT-PCR, mean ± SEM. Two-way ANOVA followed by the Newman–Keuls test, $^{*}p < 0.05$, $^{**}p < 0.01$, $^{****}p < 0.0001$ vs. 22 °C

observed in AgRP$^{\Delta GHR}$ male mice (Supplementary Fig. 4). These data are in agreement with previous findings showing that short-term, but not long-term, exposure to thermoneutrality suppressed the activation of AgRP neurons [25, 26]. The number of cFos^{+} neurons in mice of both genotypes housed at 30 °C was similar to that measured at 22 °C (Fig. 4B and Supplementary Fig. 4B).

BAT transcriptome in thermoneutrality in middle-aged female AgRP$^{\Delta GHR}$ mice

We next assessed the impact of GHR deletion from AgRP neurons on BAT transcriptome in animals adapted to thermoneutrality for 3 days as compared to animals housed at room temperature. A total of 51 genes were changed in BAT by 30 °C in female AgRP$^{\Delta GHR}$ mice, compared to 101 genes in control mice (FDR < 0.05, Fig. 5A), suggesting different mechanisms of adaptation. The regulated pathways for control and AgRP$^{\Delta GHR}$ female mice are shown in the Supplementary Material. Female AgRP$^{\Delta GHR}$ mice were less responsive to thermoneutrality, with reduced changes in pathways when adapted from 22 to 30 °C (Fig. 5B). Surprisingly, we identified several lipid metabolic pathways that were uniquely downregulated in control animals in adaptation to thermoneutrality and in AgRP$^{\Delta GHR}$ compared to control mice at 22 °C (Fig. 5B). Specifically, lipid biosynthesis, glycerolipid metabolism, and lipid oxidation pathways were among those uniquely downregulated in control animals in adaptation from 22 to 30 °C. In the AgRP$^{\Delta GHR}$ female mice, these pathways were already downregulated at 22 °C and did not change with adaptation from 22 to 30 °C (Fig. 5B, C). Among the common genes downregulated in both control and AgRP$^{\Delta GHR}$ mice by adaptation to thermoneutrality were metabolic genes *Gk*, *Dio2*, *Ucp3*, *Ucp1*, and *Ankrd9* (Fig. 5D). Importantly, the genes associated with lipid accumulation and glucose regulation (*Malat1*, *Ankrd9*, *Kcnq1ot1*, *Slc12a2*, *Peg3*) which were downregulated only in female controls in adaptation to 30 °C were also downregulated in female AgRP$^{\Delta GHR}$ mice at 22 °C compared to control mice (Fig. 5E, F). These genes were not changed in the female AgRP$^{\Delta GHR}$ mice in adaptation to 30 °C (Fig. 5F), suggesting the role of GHR in AgRP neurons for the adaptation of BAT lipid and glucose metabolism to environmental temperatures.

Discussion

We identified a unique role for GHR signaling in hypothalamic AgRP neurons in controlling thermal adaptation. Using previously characterized AgRP-specific GHR knockout mice [18], we show that GHR signaling in AgRP neurons regulates body core temperature in female, but not in male, mice. Importantly, middle-aged female AgRP$^{\Delta GHR}$ mice show impaired adaptation to cold or thermoneutrality with increased BAT lipid accumulation and aberrant transcriptomic signatures. Specifically, female AgRP$^{\Delta GHR}$ mice exhibited transcriptomic signatures of downregulated lipid metabolic genes that are similar to those of female controls adapting to temperature change. This indicates that GHR signaling mediates the response to thermoneutrality in the AgRP neurons in a sex-specific manner.

The ARC is a major site for the integration of multiple nutritional and hormonal signals, which are central to the modulation of energy balance and temperature homeostasis [27]. Evidence for the importance of GH-responsive neurons in the hypothalamus in energy homeostasis and nutrient deprivation was previously reported [18, 28–30]. Moreover, the orexigenic effect of GH signaling is possibly mediated by AgRP neurons, since most of the AgRP/NPY neurons express GHR, and AgRP-specific GHR knockout mice are unable to adapt to food restriction and maintained a higher energy expenditure, having increased weight loss during food restriction compared to the

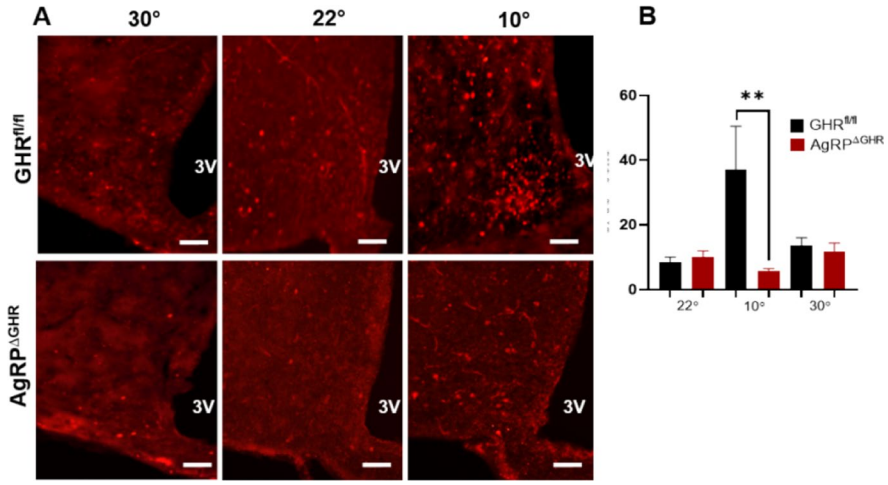

Fig. 4 Cold exposure activates ARC neurons in control, but not in AgRPP$^{\Delta GHR}$P female mice. **A** Representative images of immunohistochemical detection of cFos (red) in the arcuate nucleus (ARC) of 12–14-month-old control and AgRP$^{\Delta GHR}$ female mice after housing at either 10 °C, 22 °C, or 30 °C. **B** Quantitation of Fos-positive cells in the ARC. Scale bar, 100 mm; $n = 3$–5 group, mean ± SEM. Two-way ANOVA followed by the Newman–Keuls test, $^{**}p < 0.01$ vs. 22 °C

control mice [17]. In support, our earlier study with young male and female AgRP$^{\Delta GHR}$ mice does not show changes in body weight, body composition, food intake, or glucose homeostasis [18]. Here, we show that despite similar body weights and activity levels, the obligatory energy expenditure required for basal activity is reduced in young AgRP$^{\Delta GHR}$ female, but not male, mice and is associated with lower body core temperature, reduced heat production, increased BAT adipocyte size, and reduced BAT expression of thermogenic genes. During the aging process, such metabolic imbalance led to a slight increase in middle-aged females' body weight, accompanied by an inability to properly respond to changes in environmental temperatures. Given a significant increase in BAT lipid accumulation, the duration of eating/fasting patterns may be different in AgRP$^{\Delta GHR}$ female mice since AgRP neurons regulate complex behavioral and physiological feeding changes [31, 32]. It is reasonable to hypothesize that age-associated decline in GH signaling in the AgRP neurons is responsible for or, importantly, contributes to the impairment in BAT thermogenic capacity occurring with age [33].

The recent work has established that in addition to negative feedback regulation of hormonal signals to nutrient intake and energy metabolism, AgRP neuron activity rapidly increases following exposure to a mild cold environment and that the activity of these neurons at thermoneutrality is lower [25]. In support, we detected activation of ARC neurons in response to cold exposure that was impaired in AgRP$^{\Delta GHR}$ mice of both sexes. No significant differences in neuronal activation in response to thermoneutrality were observed. Exposure to a warm environment was shown to suppress AgRP activity in 10-day-old pups [26]. A recent study demonstrated that the control of BAT thermogenesis by AgRP neurons is independent of environmental temperature and activation of thermoregulation since specific activation of AgRP neurons suppresses BAT thermogenic activity [34]. Specifically, in mice maintained in the thermoneutral zone of 30 °C, the effects of AgRP neuronal activation on BAT temperature, energy expenditure, and locomotor activity were significantly reduced. Moreover, during cold exposure, chemogenetic activation of AgRP neurons reduced BAT temperature to a similar extent as at ambient temperature, providing evidence for the AgRP-BAT circuit independent of environmental temperature and cold-induced thermoregulation. This effect was mediated via hypothalamic mTOR complex 1 (mTORC1) signaling [34].

Middle-aged AgRP$^{\Delta GHR}$ female mice exhibit reduced body core temperature regardless of environmental temperature (22 °C, 10 °C, or 30 °C), suggesting that GHR signaling in the AgRP neurons can sense energy availability and AgRP activity related to

the AgRP-BAT circuit. mTORC1 activity is indeed lower in multiple organs of Snell dwarf and global GHR KO mice [35], suggesting a requirement for this mechanism and properly regulated GHR signaling in AgRP neurons for thermogenic action. Indeed, we found downregulation of mTOR signaling in control BAT, but not in the BAT of AgRP$^{\Delta GHR}$ female mice. Further insights on the regulation of the mTORC1 pathway in the AgRP neurons lacking GHR signaling would be informative to establish the role of this circuit in the regulation of body core temperature in aging.

Our new data provide a critical insight into the sexual dimorphism of GHR signals in AgRP neurons in thermoregulation. Sex-specific differences in body core temperature were previously reported. Body core temperature was overall higher in C57Bl/6 J female mice than in male mice throughout the adult lifetime [23]. Similarly, we observed higher body core temperature in female control mice compared to male mice. Upon exposure to the cold or warm environment, adult female AgRP$^{EYFP\Delta GHR}$ mice exhibited a significantly lower body core temperature compared to controls, while male AgRP$^{\Delta GHR}$ mice adapted to changes in environmental temperatures similar to male controls. While unexpected, a similar sex-specific phenotype was shown in female mice lacking CRFR1 in AgRP neurons [11]. Only female mice selectively lacking CRFR1 in AgRP neurons exhibited reduced heat production and lower body temperature, followed by a maladaptive thermogenic response to cold. In the ARC, the GHR gene is co-expressed with CRFR in the same cluster of AgRP neurons [36], suggesting a sex-specific role of this subpopulation of AgRP neurons in energy homeostasis and regulation of body core temperature. Additionally, a sex-specific phenotype was observed in female mice lacking leptin receptors in POMC neurons or AgRP neurons, which, as in AgRP$^{\Delta GHR}$ and AgRP$^{\Delta CRFR1}$ female mice, exhibited reduced heat production with unaltered food intake [37, 38]. There is some evidence that estrogen modulates GH action independent of secretion [39]. While estrogen receptor is not expressed by AgRP neurons [40], estrogen can directly affect GHR expression and signaling [39]. Sex hormones were proposed to influence body core temperature by direct action on neurons in the POA of the hypothalamus that express the receptors for testosterone and estrogen [41]. AgRP neurons have been shown to project to the POA, suggesting the connections between AgRP neurons and the POA in the regulation of resting energy expenditure [42]. Interestingly, gonadectomy elevated body core temperature in male, but not in female, mice [23], suggesting gonadal-dependent modulation of thermoregulation. It is important to note that within each sex, the levels of GH were unaltered in AgRP$^{\Delta GHR}$ mice, while phosphorylation of STAT5 was significantly reduced [17, 18]. Our new studies thus provide a critical view of the sex-specific role of GHR signaling in AgRP neurons in thermoregulation with particular importance for adult animals. Future studies will be required to assess the effect of sex hormones and their interaction with GH on sex-specific differences observed in our study.

Transcriptomic analysis of BAT demonstrated that genes associated with lipid metabolic processes and lipid accumulation were downregulated in AgRP$^{\Delta GHR}$ female mice compared to the control. Moreover, these were the same genes downregulated by thermoneutrality in control mice but not in the AgRP$^{\Delta GHR}$ animals. The divergent response of BAT in the AgRP$^{\Delta GHR}$ female mice was evident by downregulation in key genes associated with lipid accumulation and glucose regulation such as *Malat1*, *Ankrd9*, *Kcnq1ot1*, *Slc12a2*, and *Peg3*. These genes were not changed in the AgRP$^{\Delta GHR}$ female mice during adaptation to 30 °C. Some of these genes, such as *Malat1*, were shown to promote hepatic steatosis and insulin resistance by modulating lipid accumulation through SREBP-1c [43], while *Ankrd9*, *Kcnq1ot1*, and *Peg3* are involved in intracellular lipid accumulation and lipogenesis [44–46], and *Slc12a2* plays a role in insulin secretion and glucose-stimulated plasma membrane depolarization [47]. Interestingly, among the genes associated with fatty acid metabolism, *Scd1* and *Scd2* were upregulated in the AgRP$^{\Delta GHR}$ female mice, indicating shifts in metabolic homeostasis and substrate utilization [48]. Interestingly, SCD1 deficiency stimulates basal thermogenesis through the upregulation of the beta-3-AR-mediated pathway and an increase in lipolysis and fatty acid oxidation in BAT [49].

A relationship between GH and thermoregulation was previously suggested. Central infusion of GH into the hypothalamus leads to an increase in sympathetic nerve activity [50, 51]. Furthermore, the inability of whole-body GHR KO mice

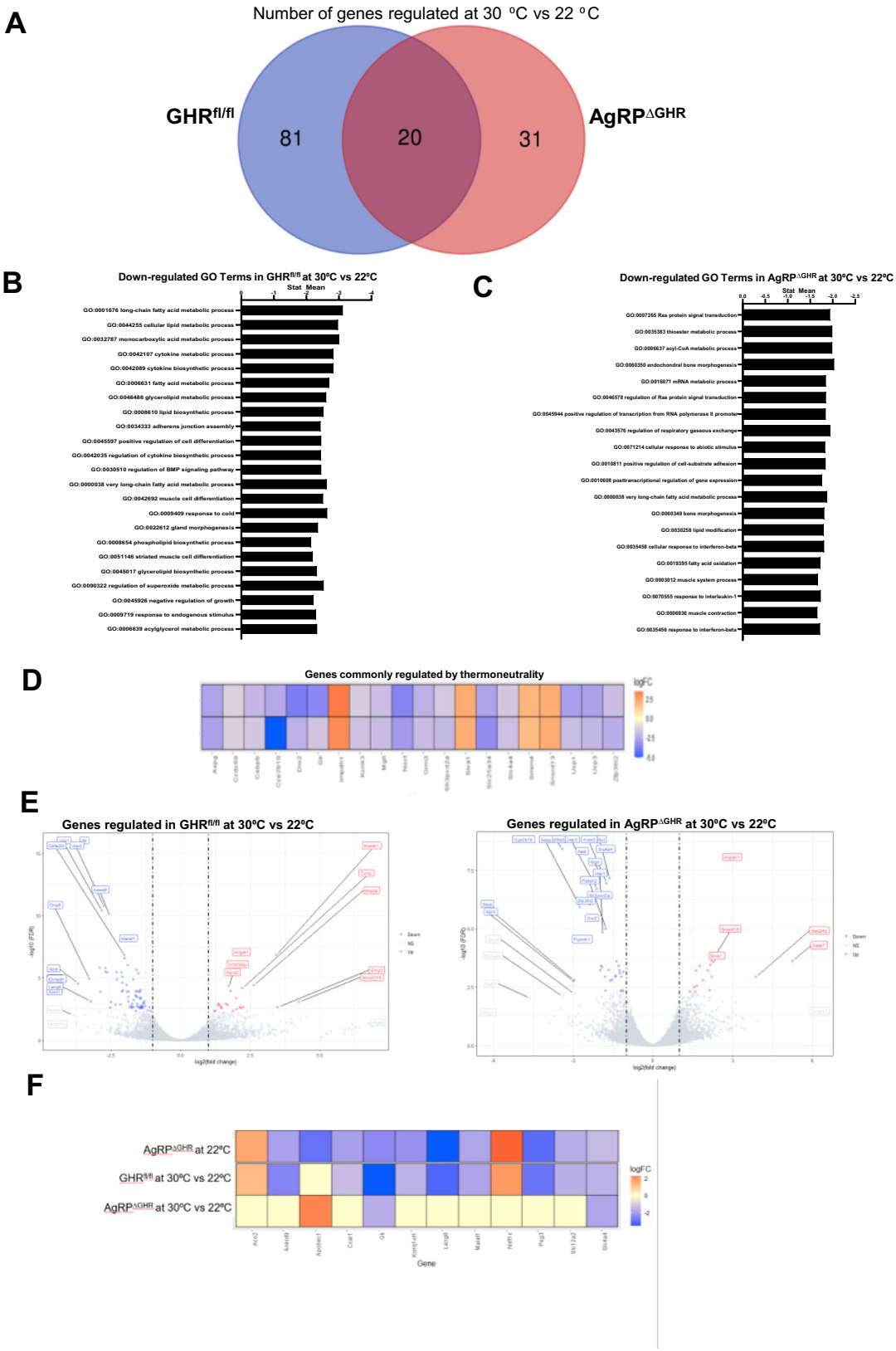
A
Number of genes regulated at 30 ºC vs 22 ºC
GHRfl/fl
81
20
31
AgRPΔGHR
B
Down-regulated GO Terms in GHRfl/fl at 30ºC vs 22ºC
Stat Mean
GO:0001676 long-chain fatty acid metabolic process
GO:0044255 cellular lipid metabolic process
GO:0032787 monocarboxylic acid metabolic process
GO:0042107 cytokine metabolic process
GO:0042089 cytokine biosynthetic process
GO:0006631 fatty acid metabolic process
GO:0046486 glycerolipid metabolic process
GO:0008610 lipid biosynthetic process
GO:0034333 adherens junction assembly
GO:0045597 positive regulation of cell differentiation
GO:0042035 regulation of cytokine biosynthetic process
GO:0030510 regulation of BMP signaling pathway
GO:0000038 very long-chain fatty acid metabolic process
GO:0042692 muscle cell differentiation
GO:0009409 response to cold
GO:0022612 gland morphogenesis
GO:0008654 phospholipid biosynthetic process
GO:0051146 striated muscle cell differentiation
GO:0045017 glycerolipid biosynthetic process
GO:0090322 regulation of superoxide metabolic process
GO:0045926 negative regulation of growth
GO:0009719 response to endogenous stimulus
GO:0006639 acylglycerol metabolic process
C
Down-regulated GO Terms in AgRPΔGHR at 30ºC vs 22ºC
Stat Mean
GO:0007265 Ras protein signal transduction
GO:0035383 thioester metabolic process
GO:0006637 acyl-CoA metabolic process
GO:0060350 endochondral bone morphogenesis
GO:0016071 mRNA metabolic process
GO:0046578 regulation of Ras protein signal transduction
GO:0045944 positive regulation of transcription from RNA polymerase II promoter
GO:0043576 regulation of respiratory gaseous exchange
GO:0071214 cellular response to abiotic stimulus
GO:0010811 positive regulation of cell-substrate adhesion
GO:0010608 posttranscriptional regulation of gene expression
GO:0000038 very long-chain fatty acid metabolic process
GO:0060349 bone morphogenesis
GO:0030258 lipid modification
GO:0035458 cellular response to interferon-beta
GO:0019395 fatty acid oxidation
GO:0003012 muscle system process
GO:0070555 response to interleukin-1
GO:0006936 muscle contraction
GO:0035456 response to interferon-beta
D
Genes commonly regulated by thermoneutrality
logFC
E
Genes regulated in GHRfl/fl at 30ºC vs 22ºC
Genes regulated in AgRPΔGHR at 30ºC vs 22ºC
Down
NS
Up
log2(fold change)
F
AgRPΔGHR at 22ºC
GHRfl/fl at 30ºC vs 22ºC
AgRPΔGHR at 30ºC vs 22ºC
logFC
Gene

◂**Fig. 5** Differentially expressed genes in AgRP$^{\Delta GHR}$ female mice exposed to thermoneutrality. **A** The Venn diagram depicts the number of overlapping genes and differentially expressed genes in the 12–14-month-old control and AgRP$^{\Delta GHR}$ female mice (left) at 30 °C versus 22 °C. **B** Downregulated functions were identified by GO analysis in female controls at 30 °C versus 22 °C. **C** Downregulated functions were identified by GO analysis in AgRP$^{\Delta GHR}$ female mice at 30 °C versus 22 °C. **D** Heatmap illustrating the relative expression of overlapping genes by 30 °C. **E** Genes regulated only in female controls (right) or only in AgRP$^{\Delta GHR}$ female mice (left) at 30 °C vs. 22 °C. **F** Heatmap illustrating the differentially expressed genes in AgRP$^{\Delta GHR}$ female mice at 22 °C vs. control, and the relative expression of unique genes at 30 °C vs. 22 °C in control and AgRP$^{\Delta GHR}$ female mice

to respond to cold exposure or β-adrenergic receptor agonist treatment suggested that GH plays an important role in thermoregulation [52]. Previous studies using whole-body GHR KO and GH-deficient Ames dwarf mice showed an increased amount of BAT [14, 53], increased expression of thermogenic genes in BAT, and thermogenic activation ("browning") of subcutaneous white adipose tissue (WAT), which can stimulate thermogenesis [54]. Intriguingly, similar to AgRP$^{\Delta GHR}$ female mice, body core temperature was reduced in these mutants [55, 56], despite increased thermogenesis and metabolic rate. Reduced body temperature has been associated with extended longevity [57]. Additionally, GH-deficient mice exposed to thermoneutrality had reduced expression of genes associated with lipid metabolism and energy expenditure, and morphological changes in BAT similar to AgRP$^{\Delta GHR}$ female mice [22]. More than 1500 genes are regulated in BAT at room temperature or thermoneutrality in global GHR KO mice [22]. When GHR KO mice were exposed to thermoneutral conditions, a greater number of genes were affected in BAT from GHR KO than control mice, with a low overlap between groups, indicating a divergent response. Similar to the global GHR KO mice, AgRP$^{\Delta GHR}$ mice showed little overlap in genes when compared to the responses of control mice to thermoneutrality. Nevertheless, 114 genes were commonly regulated in response to thermoneutrality by global GHR KO and AgRP$^{\Delta GHR}$ mice. Among the pathways regulated by these common genes, lipid metabolic process, fatty acid metabolic process, response to cold, and brown fat cell differentiation were the top-regulated GO terms [22]. Similar to AgRP$^{\Delta GHR}$ mice, *Ankrd9* was upregulated in GHR KO mice at 22 °C but downregulated in GHR KO mice exposed to thermoneutral conditions [22]. On the other hand, *Peg3* was upregulated in GHR KO compared to WT mice at 22 °C, while *Slc12a2* and *Scd1* were downregulated in GHR KO mice exposed to thermoneutrality [22], reflecting the differences between both models. Additional work will be required to define the common and divergent responses between these models in the regulation of body core temperature and energy homeostasis.

Aging is associated with an attenuated physiological ability to maintain body core temperature, and the risk of heat-related illness in these individuals is elevated [58]. The role of sex and reproductive hormones in thermoregulation is complex and depends on the situation, overall health, and age [59]. Our data provide evidence that GHR signaling in the AgRP neurons mediates the response to thermoneutrality, controlling the steady-state temperature in female animals. The limitation of our study is that we assessed body core temperature only in young and middle-aged mice. It is reasonable to hypothesize that during the aging process, there might be further shift in thermoregulation which will ultimately affect the metabolic health of these animals. Future studies would be required to define the impact of low body core temperature in AgRP$^{\Delta GHR}$ female mice on longevity and metabolic health in aging.

Author contribution LS, JBML, and LKD carried out the research and reviewed the manuscript. MK and LK assisted in the data collection and experimental design. JJK contributed the GHR floxed mice. AS and AB analyzed the data and reviewed the manuscript. MS designed the study, analyzed the data, wrote the manuscript, and is responsible for the integrity of this work. All authors approved the final version of the manuscript.

Funding This study was supported by the American Diabetes Association grant #1-lB-IDF-063, a Feasibility Grant from the Michigan Diabetes Research Center (P30DK020572) NIDDK, and MICP Core and metabolic core (P30DK020572) NIDDK and WSU funds for MS. LK was supported by NIH 5T32GM14519-01, and LS was supported by NIH 5T32HL120822-09.

Data availability The data that support the findings of this study are available from the corresponding author upon reasonable request.

Declarations

Competing interests The authors declare no competing interests.

References

1. Mattson MP. Perspective: does brown fat protect against diseases of aging? Ageing Res Rev. 2010;9(1):69–76.
2. Roh E, Kim MS. Brain regulation of energy metabolism. Endocrinol Metab (Seoul). 2016;31(4):519–24.
3. Robertson SA, Leinninger GM, Myers MG Jr. Molecular and neural mediators of leptin action. Physiol Behav. 2008;94(5):637–42.
4. Belgardt BF, Bruning JC. CNS leptin and insulin action in the control of energy homeostasis. Ann N Y Acad Sci. 2010;1212:97–113.
5. Van Someren EJ. Thermoregulation and aging. Am J Physiol Regul Integr Comp Physiol. 2007;292(1):R99-102.
6. Osilla EV, JL Marsidi, S Sharma, Physiology, temperature regulation. StatPearls. 2022: Treasure Island (FL).
7. Rosenbaum M, Leibel RL. Adaptive thermogenesis in humans. Int J Obes (Lond). 2010;34(Suppl 1):S47-55.
8. Chong AC, Greendyk RA, Zeltser LM. Distinct networks of leptin- and insulin-sensing neurons regulate thermogenic responses to nutritional and cold challenges. Diabetes. 2015;64(1):137–46.
9. Han Y, et al. Deciphering an AgRP-serotoninergic neural circuit in distinct control of energy metabolism from feeding. Nat Commun. 2021;12(1):3525.
10. Yu S, et al. The hypothalamic preoptic area and body weight control. Neuroendocrinol. 2018;106(2):187–94.
11. Kuperman Y, et al. CRFR1 in AgRP neurons modulates sympathetic nervous system activity to adapt to cold stress and fasting. Cell Metab. 2016;23(6):1185–99.
12. Bartke A, Brown-Borg H. Life extension in the dwarf mouse. Curr Top Dev Biol. 2004;63:189–225.
13. Waters MJ, et al. New insights into growth hormone action. J Mol Endocrinol. 2006;36(1):1–7.
14. Darcy J, et al. Brown adipose tissue function is enhanced in long-lived, male Ames dwarf mice. Endocrinol. 2016;157(12):4744–53.
15. Darcy J, et al. Increased environmental temperature normalizes energy metabolism outputs between normal and Ames dwarf mice. Aging (Albany NY). 2018;10(10):2709–22.
16. Westbrook R, et al. Alterations in oxygen consumption, respiratory quotient, and heat production in long-lived GHRKO and Ames dwarf mice, and short-lived bGH transgenic mice. J Gerontol A Biol Sci Med Sci. 2009;64(4):443–51.
17. Furigo IC, et al. Growth hormone regulates neuroendocrine responses to weight loss via AgRP neurons. Nat Commun. 2019;10(1):662.
18. de Lima JBM, et al. Hypothalamic GHR-SIRT1 axis in fasting. Cells. 2021; 10(4).
19. List EO, et al. Liver-specific GH receptor gene-disrupted (LiGHRKO) mice have decreased endocrine IGF-I, increased local IGF-I, and altered body size, body composition, and adipokine profiles. Endocrinol. 2014;155(5):1793–805.
20. Sadagurski M, Cady G, Miller RA. Anti-aging drugs reduce hypothalamic inflammation in a sex-specific manner. Aging Cell. 2017;16(4):652–60.
21. Sadagurski M, et al. Human IL6 enhances leptin action in mice. Diabetologia. 2010;53(3):525–35.
22. Schneider A, et al. Growth hormone signaling shapes the impact of environmental temperature on transcriptomic profile of different adipose tissue depots in male mice. J Gerontol: Series A. 2021;77(5):941–6.
23. Sanchez-Alavez M, Alboni S, Conti B. Sex- and age-specific differences in core body temperature of C57Bl/6 mice. Age (Dordr). 2011;33(1):89–99.
24. Klein Hazebroek M, Keipert S. Adapting to the cold: a role for endogenous fibroblast growth factor 21 in thermoregulation? Front Endocrinol (Lausanne). 2020;11:389.
25. Deem JD, et al. Cold-induced hyperphagia requires AgRP neuron activation in mice. Elife. 2020;9.
26 Zimmer MR, et al. Functional ontogeny of hypothalamic Agrp neurons in neonatal mouse behaviors. Cell. 2019;178(1):44–59 (**e7**).
27. Timper K, Bruning JC. Hypothalamic circuits regulating appetite and energy homeostasis: pathways to obesity. Dis Model Mech. 2017;10(6):679–89.
28. de Lima JBM, et al. ARCGHR neurons regulate muscle glucose uptake. Cells. 2021;10(5):1093.
29. Furigo IC, et al. Growth hormone enhances the recovery of hypoglycemia via ventromedial hypothalamic neurons. FASEB J. 2019; fj201901315R.
30. Wasinski F, et al. Growth hormone receptor deletion reduces the density of axonal projections from hypothalamic arcuate nucleus neurons. Neurosci. 2020;434:136–47.
31. Dietrich MO, et al. Hypothalamic Agrp neurons drive stereotypic behaviors beyond feeding. Cell. 2015;160(6):1222–32.
32. Cavalcanti-de-Albuquerque JP, et al. Regulation of substrate utilization and adiposity by Agrp neurons. Nat Commun. 2019;10(1):311.
33. Graja A, Schulz TJ. Mechanisms of aging-related impairment of brown adipocyte development and function. Gerontol. 2015;61(3):211–7.
34. Burke LK, et al. mTORC1 in AGRP neurons integrates exteroceptive and interoceptive food-related cues in the modulation of adaptive energy expenditure in mice. Elife. 2017;6.
35. Dominick G, et al. Regulation of mTOR activity in Snell dwarf and GH receptor gene-disrupted mice. Endocrinol. 2015;156(2):565–75.
36. Campbell JN, et al. A molecular census of arcuate hypothalamus and median eminence cell types. Nat Neurosci. 2017;20(3):484–96.
37. Shi H, et al. Sexually different actions of leptin in proopiomelanocortin neurons to regulate glucose homeostasis. Am J Physiol Endocrinol Metab. 2008;294(3):E630–9.
38. van de Wall E, et al. Collective and individual functions of leptin receptor modulated neurons controlling metabolism and ingestion. Endocrinol. 2008;149(4):1773–85.
39. Leung KC, et al. Estrogen regulation of growth hormone action. Endocr Rev. 2004;25(5):693–721.

40. Olofsson LE, Pierce AA, Xu AW. Functional requirement of AgRP and NPY neurons in ovarian cycle-dependent regulation of food intake. Proc Natl Acad Sci U S A. 2009;106(37):15932–7.
41. Kruijver FP, Swaab DF. Sex hormone receptors are present in the human suprachiasmatic nucleus. Neuroendocrinol. 2002;75(5):296–305.
42. Morselli LL, et al. Control of energy expenditure by AgRP neurons of the arcuate nucleus: neurocircuitry, signaling pathways, and angiotensin. Curr Hypertens Rep. 2018;20(3):25.
43. Yan C, Chen J, Chen N. Long noncoding RNA MALAT1 promotes hepatic steatosis and insulin resistance by increasing nuclear SREBP-1c protein stability. Sci Rep. 2016;6:22640.
44. Wang X, et al. Regulation of ANKRD9 expression by lipid metabolic perturbations. BMB Rep. 2009;42(9):568–73.
45. Yu XH, et al. LncRNA kcnq1ot1 promotes lipid accumulation and accelerates atherosclerosis via functioning as a ceRNA through the miR-452-3p/HDAC3/ABCA1 axis. Cell Death Dis. 2020;11(12):1043.
46. Ghimire S, Kim J. PEG3 controls lipogenesis through ACLY. PLoS One. 2021;16(5):e0252354.
47. Alshahrani S, et al. Increased Slc12a1 expression in beta-cells and improved glucose disposal in Slc12a2 heterozygous mice. J Endocrinol. 2015;227(3):153–65.
48. Flowers MT, Ntambi JM. Role of stearoyl-coenzyme A desaturase in regulating lipid metabolism. Curr Opin Lipidol. 2008;19(3):248–56.
49. Lee SH, et al. Lack of stearoyl-CoA desaturase 1 upregulates basal thermogenesis but causes hypothermia in a cold environment. J Lipid Res. 2004;45(9):1674–82.
50. Tran LT, et al. Hypothalamic control of energy expenditure and thermogenesis. Exp Mol Med. 2022;54(4):358–69.
51. Yasuda T, et al. Centrally administered ghrelin suppresses sympathetic nerve activity in brown adipose tissue of rats. Neurosci Lett. 2003;349(2):75–8.
52. Nelson CN, et al. Growth hormone activated STAT5 is required for induction of beige fat in vivo. Growth Horm IGF Res. 2018;42–43:40–51.
53. Li Y, Knapp JR, Kopchick JJ. Enlargement of interscapular brown adipose tissue in growth hormone antagonist transgenic and in growth hormone receptor gene-disrupted dwarf mice. Exp Biol Med (Maywood). 2003;228(2):207–15.
54. Desai BN, Harris RB. Integrated effects of leptin in the forebrain and hindbrain of male rats. Endocrinol. 2013;154(8):2663–75.
55. Hunter WS, et al. Low body temperature in long-lived Ames dwarf mice at rest and during stress. Physiol Behav. 1999;67(3):433–7.
56. Hauck SJ, et al. Reduced levels of thyroid hormones, insulin, and glucose, and lower body core temperature in the growth hormone receptor/binding protein knockout mouse. Exp Biol Med (Maywood). 2001;226(6):552–8.
57. Conti B, et al. Transgenic mice with a reduced core body temperature have an increased life span. Science. 2006;314(5800):825–8.
58. Waalen J, Buxbaum JN. Is older colder or colder older? The association of age with body temperature in 18,630 individuals. J Gerontol A Biol Sci Med Sci. 2011;66(5):487–92.
59. Yanovich R, Ketko I, Charkoudian N. Sex differences in human thermoregulation: relevance for 2020 and beyond. Physiol. 2020;35(3):177–84.